

Assessment of metastatic capacity in *in vitro* models of skin and cervical cancer using spheroids

Daniel F. Arévalo P. *, David S. Sánchez L. †, Joel Frayle M. ‡ Oscar A. Nontoa N. §

Department of Biomedical Engineering, Universidad de los Andes. Bogotá, Colombia

Email: *darevalop@uniandes.edu.co, †ds.sanchez11@uniandes.edu.co, ‡j.frayle@uniandes.edu.co,
§o.nontoa@uniandes.edu.co

Abstract—Different approaches have been developed for the treatment of cancer, a disease in which some cells in the body proliferate uncontrollably and spread to other parts of the body. Both skin cancer and cervical (uterine cervix) cancer have high worldwide incidence and are triggered by multiple associated factors. One commonly used model to evaluate cancer treatments is spheroid formation. The advantage of tumor spheroids as an *in vitro* biological model is that they can mimic the 3D structure of avascular primary tumors. Therefore, the aim of this project is to determine the metastatic capacity of skin and cervical cancer tumors as a function of the diameter of their necrotic core in an *in vitro* model.

Keywords: Spheroids, necrotic core, HaCaT, HeLa.

I. INTRODUCTION

Spheroids are three-dimensional multicellular aggregates that display physiological characteristics closer to their tissue of origin compared to 2D cell cultures [1]. One of their main uses is their ability to function as *in vitro* models of avascular solid tumors, allowing observation of necrotic core formation [4]. This necrotic core is important because it reflects the degree of hypoxia experienced by the tumor mass and its size—both factors that influence the onset of metastasis [5]. It has been shown that a larger proliferative zone has a higher probability of detaching cells or groups of cells from the spheroid; therefore, a larger proliferative zone is more likely to release cancer cells into the bloodstream and trigger metastasis in different organs of the patient [2]. However, the probability of metastasis also depends on the cell type, since a very rapid development of a necrotic core can lead to a tumor with different properties regarding its expansion to other parts of the body. For example, in the brain and lungs, the larger the tumor, the higher the probability of metastasis, whereas in the liver the tumor size with the highest probability of metastasis occurs between 3 and 7 centimeters [3].

Non-melanoma skin cancer is the most frequent type of cancer globally, with an incidence of 253.2 people per 100,000 per year and a high capacity to generate metastasis [6]. This is likely due to prolonged exposure to UV radiation, either for occupational or recreational reasons [7]. In addition, an increase in mortality of 122% has been reported since 2001 [6]. On the other hand, cervical cancer is the fourth most common cancer in women globally, with an incidence of 13.3 women per 100,000 [8]. It has been reported with higher incidence in less developed countries due to the lack of vaccination against human papillomavirus (HPV); the mortality rate in

these countries can be up to 18 times higher than in more developed countries [9]. It has been reported that, during the development of the primary tumor, there is a propensity to generate metastasis [10].

Based on the above, the research question is posed: How does the necrotic core of spheroids influence cell proliferation in an *in vitro* model of HaCaT and HeLa cells? The objective is to determine the metastatic capacity of skin and cervical cancer tumors as a function of necrotic core diameter in an *in vitro* model. To achieve this general objective, we propose to analyze the distribution of the necrotic core in the HeLa cell line (cervical cancer) and in the HaCaT cell line (skin cancer). In addition, we propose to relate necrotic core distributions with the proliferative capacity of the cancer types under study.

II. METHODOLOGY

Because HeLa and HaCaT cultures correspond to adherent cells, the detachment of the monolayer must first be performed. For this, 5 mL of culture medium were removed, followed by a wash with PBS of the same volume; the suspension was homogenized and removed. For detachment, 2 mL of trypsin were applied to the monolayer and incubated for 1 minute. However, for keratinocytes (HaCaT), both the trypsin volume and incubation time required for detachment were greater than those used for HeLa cultures.

Next, cell detachment was checked and 5 mL of fresh DMEM medium were added to inhibit trypsin. The flask surface was resuspended and transferred to a 15 mL Falcon tube, which was centrifuged for 5 minutes at 1800 rpm to obtain the cell pellet. When only 1 mL of medium remained, 10 μ L of the suspension were taken and added to 90 μ L of Trypan Blue. From this solution, 10 μ L were taken to perform cell counting in a Neubauer chamber.

The seeding process considered the previous cell count and adjusted cell density to three different levels: 100,000 cells/mL, 150,000 cells/mL, and 200,000 cells/mL for both HeLa and HaCaT. Seeding for each density was performed in triplicate in an SPL Life Sciences microplate.

Finally, the resulting microplate was placed on a microplate shaker for 20 minutes at 60 rpm and then incubated at 37°C and 5% CO₂ to record photographic documentation on different days. The procedures used for spheroid formation can be seen in Figure 1 and Figure 2.

A. Cell preparation and counting

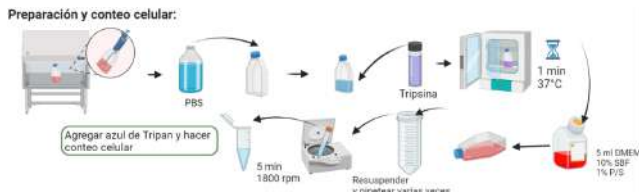


Figure 1: Schematic of the protocol used for cell counting in culture.

B. Cell density adjustment and microplate seeding

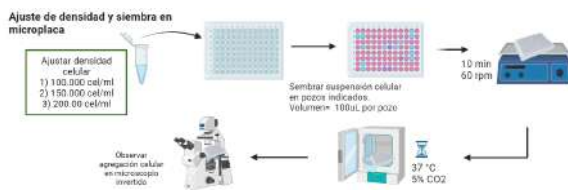


Figure 2: Schematic of the protocol used for spheroid formation.

III. RESULTS

Figure 3 shows the distribution of HaCaT cells immediately after seeding in the microplate. The cells show a circular distribution, and cell density depends on the concentration seeded: higher concentrations yield a larger occupied area of the microplate. All images correspond to 4X magnification.

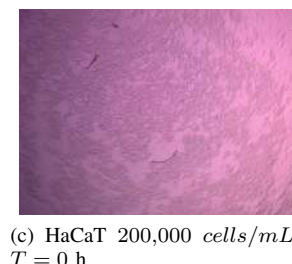
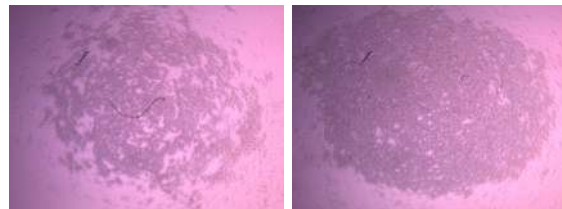


Figure 3: T = 0 h, HaCaT cells

Figure 4 again shows the distribution of HaCaT cells, but this time with a larger occupied area in the microplate. These images were taken 120 hours after seeding and correspond to 4X magnification. In this distribution, spaces between cells can be seen, indicating that cells are well distributed and there is no major aggregation, except in Figure 4a, where a darker

region appears in the center of the formation, indicating cell adherence in that area.

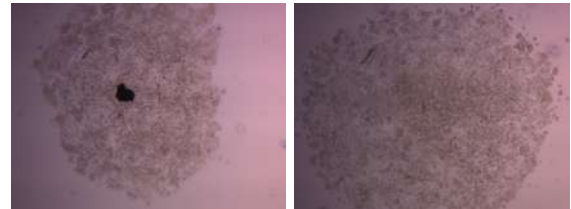


Figure 4: T = 120 h, HaCaT cells

Figure 5 shows the distribution of HeLa cells immediately after seeding in the microplate. Again, a distribution with a circular tendency can be observed, where the number of cells present and the microplate area occupied increase as a function of the seeded concentration.

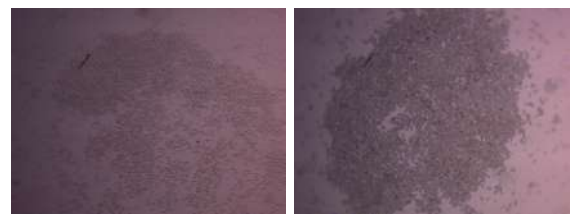
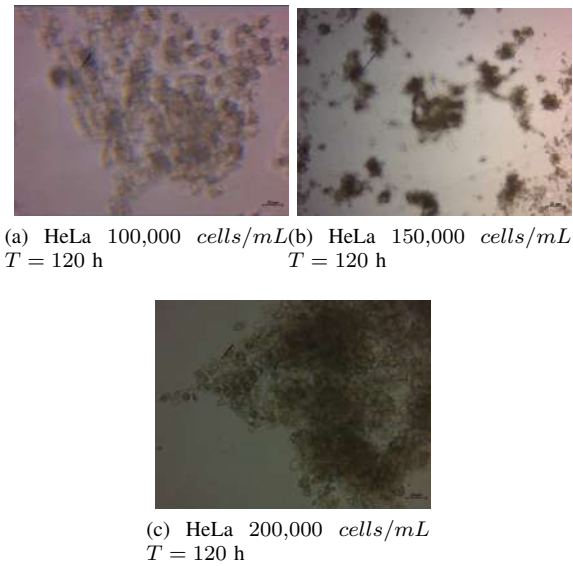


Figure 5: T = 0 h, HeLa cells

Figure 6 shows HeLa cell distributions after 120 hours. In this case, the initial circular distribution has been lost, and darker regions can be observed but without a defined shape. The image that most preserves a circular appearance is Figure 6c; however, it also presents regions with low cell presence inside the formation.

Figure 6: $T = 120$ h, HeLa cells

IV. RESULTS ANALYSIS

In Figures 3a, 3b and 3c, it is possible to observe HaCaT cells after being seeded in the microplate. As can be seen, the cell density with the most uniform circular geometry at time 0 is the 150,000 cells/mL condition, followed by 100,000 cells/mL, while the 200,000 cells/mL condition shows the lowest uniformity at the initial time. These initial differences may be due to several factors; one of them, for example, is the way each well was resuspended. This is because the highest concentration is the one showing the least accumulation in the center of the well, so it would be possible to theorize that this concentration received the least resuspension.

In Images 4a, 4b and 4c, it is possible to observe HaCaT cells after 120 hours in the microplate. As can be seen, cell growth occurred in all concentrations; however, the photos at this time were captured with the 4X objective and it was not possible to capture the full geometry of the formations as in the initial time point. Likewise, in Figure 4a, a black spot can be observed in the center of the image that is not present in the other concentrations. As will be explained in more detail below, this spot would correspond to an accumulation of HaCaT cells.

In Figures 5a, 5b and 5c, HeLa cells can be observed at time $T = 0$ h. As can be seen in these images, the concentration that shows the most circular geometry at the initial moment is 150,000 cells/mL, followed by 200,000 cells/mL, while 100,000 cells/mL shows the lowest consistency at the initial time. In this case, these differences would again stem from the resuspension process mentioned above.

In Figures 6a, 6b and 6c, HeLa cells at different concentrations can be observed after incubating them in the microplate for 120 hours. As can be seen in these images, none of the concentrations formed structures with geometries similar to spheroids; on the contrary, the circular structure present at time 0 was destroyed, leaving cells dispersed throughout the well and generating structures without uniform shapes, as observed for the 100,000 cells/mL and 200,000 cells/mL conditions.

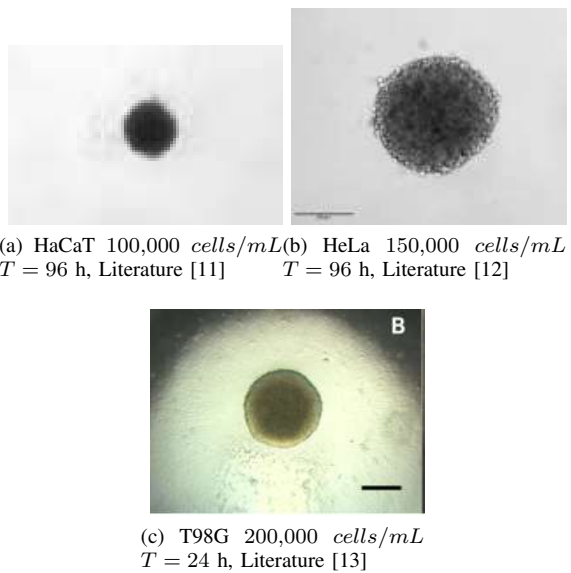


Figure 7: Comparison with literature for different cell lines

In Figures 7a, 7b and 7c, spheroids of HaCaT, HeLa and T98G cells can be observed. These images show what a spheroid looks like in different cell lines (Figures 7a and 7b) and also allow comparison with other spheroidal conformations (Figure 7c). When comparing our results with the literature, it is possible to observe that the conformations obtained do not match what is expected. This can be stated because, first, the structures obtained are not three-dimensional and, instead, only a 2D sheet of cells is observed. Likewise, it is also possible to observe that literature spheroids have higher accumulation in the center of the structures, whereas in the results obtained by the research team, cells did not reach that level of closeness. In addition, after 120 hours it is still possible to observe spaces between the cells, which are not present in the literature.

These results may be due to multiple factors. One of them, for example, is that the SPL Life Sciences plate used did not have the low-adhesion properties required to prevent cells from adhering to the plate. Therefore, having sufficient adhesion for cells to attach to the plate prevented them from forming cell-cell unions. Another factor that was not considered is that these plates sometimes require a matrix at the bottom of the microplate when working with adherent cell lines such as those used here [14]. Therefore, in future experiments, to test this hypothesis, the SPL plate could be replaced with a Corning plate, which was used in the study of spheroids with T98G cells [14].

Additional possible causes of adhesion in this experiment have also been proposed, including the fact that HaCaT cells are not transformed, which may imply low cell-cell adhesion and increase the need to adhere to the microplate. In addition, it has been documented in the literature that for highly adherent cells such as HaCaT, using other containers instead of microplates—such as microbubbles—can be more efficient, since the material is designed to be removed while leaving the spheroid intact. Human error during seeding is also common, such as touching the edges or bottom of the microplate, which

can cause the material to lose its low-adhesion properties. Another possible option is the use of cell strainers to limit cell adherence to the plate [15], [16].

V. CONCLUSIONS

From the laboratory work, it can be concluded that the proposed objectives could not be achieved due to errors in the selection of the low-adhesion microplate, which prevented spheroid formation for HeLa and HaCaT. Therefore, there was no necrotic core or proliferative zone formation in the spheroids.

However, higher proliferation was observed in HaCaT cells compared to HeLa cells, indicating that skin cancer may have faster growth than cervical cancer. In a future experiment, the type of microplate used (low-adhesion) should be strictly considered, and a microbubble-based process could even be used to prevent cell adherence to the base.

Spheroid formation can be corroborated through confocal microscopy to observe distinct zones (necrotic, quiescent, and proliferative) and necrotic core size. Finally, it is recommended to keep a longer photographic record of spheroid observations to evidence cell detachment and obtain a closer approximation to the ability of these cells to generate metastasis.

REFERENCES

- [1] Y. Park et al., “Three-dimensional, multifunctional neural interfaces for cortical spheroids and engineered assembloids,” *Sci. Adv.*, vol. 7, no. 12, pp. 9153–9170, Mar. 2021, doi: 10.1126/SCI-ADV.ABF9153/SUPPL_FILE/ABF9153_SM.PD
- [2] Y. Klm and H. G. Othmer, “HYBRID MODELS OF CELL AND TISSUE DYNAMICS IN TUMOR GROWTH,” *HHS Public Access*, 2015, doi: 10.3934/mbe.2015.12.1141.
- [3] Q. Shan, Y. Fan, J. Guo, X. Han, H. Wang, and Z. Wang, “Relationship between tumor size and metastatic site in patients with stage IV non-small cell lung cancer: A large SEER-based study,” *PeerJ*, vol. 2019, no. 10, 2019, doi: 10.7717/peerj.7822.
- [4] S. Daunys, A. Janonienė, I. Januškevičienė, M. Paškevičiūtė, and V. Petrikaitė, “3D Tumor Spheroid Models for In Vitro Therapeutic Screening of Nanoparticles,” *Adv. Exp. Med. Biol.*, vol. 1295, pp. 243–270, 2021, doi: 10.1007/978-3-030-58174-9_11/FIGURES/13.
- [5] R. Leek, D. R. Grimes, A. L. Harris, and A. McIntyre, “Methods: Using three-dimensional culture (spheroids) as an *in vitro* model of tumour hypoxia,” *Adv. Exp. Med. Biol.*, vol. 899, pp. 167–196, 2016, doi: 10.1007/978-3-319-26666-4_10/FIGURES/7.
- [6] C. Alonso-Belmonte, T. Montero-Vilchez, S. Arias-Santiago, and A. Buendía-Eisman, “Current State of Skin Cancer Prevention: A Systematic Review,” *Actas Dermosifiliogr.*, vol. 113, no. 8, pp. T781–T791, Sep. 2022, doi: 10.1016/J.AD.2022.04.018.
- [7] Z. Apalla, D. Nashan, R. B. Weller, and X. Castellsagué, “Skin Cancer: Epidemiology, Disease Burden, Pathophysiology, Diagnosis, and Therapeutic Approaches,” *Dermatol. Ther. (Heidelb.)*, vol. 7, no. 1, pp. 5–19, Jan. 2017, doi: 10.1007/S13555-016-0165-Y/TABLES/2.
- [8] A. D. Shrestha et al., “Cervical cancer screening utilization, and associated factors, in Nepal: a systematic review and meta-analysis,” *Public Health*, vol. 210, pp. 16–25, Sep. 2022, doi: 10.1016/J.PUHE.2022.06.007.
- [9] P. A. Cohen, A. Jhingran, A. Oaknin, and L. Denny, “Cervical cancer,” *Lancet*, vol. 393, no. 10167, pp. 169–182, Jan. 2019, doi: 10.1016/S0140-6736(18)32470-X.
- [10] J. yan Wang and L. juan Chen, “The role of miRNAs in the invasion and metastasis of cervical cancer,” *Biosci. Rep.*, vol. 39, no. 3, Mar. 2019, doi: 10.1042/BSR20181377/111055.
- [11] P. Salmenperä, P. R. Karhemo, K. Räsänen, P. Laakkonen, A. Vaheri, Fibroblast spheroids as a model to study sustained fibroblast quiescence and their crosstalk with tumor cells. *Experimental Cell Research*, 17–24, 2016.
- [12] M. D. Crnogorac et al., 3D HeLa spheroids as a model for investigating the anticancer activity of Biginelli-hybrids. *Chemico-Biological Interactions*. 345, 2021.
- [13] D. Salazar et al., Multicellular spheroids as a model for drug evaluation in the treatment of glioblastoma multiforme, Department of Biomedical Engineering, Universidad de los Andes, pp. 1-9, 2020.
- [14] S. Chandrasekaran, U.-B. T. Giang, M. R. King, and L. A. Delouise, doi: 10.1016/j.biomaterials.2011.06.013. “Spheroid Models: Getting Started and Culture Tips.”, 2020.
- [15] S. Chandrasekaran, U.-B. T. Giang, M. R. King, and L. A. Delouise, “Microenvironment induced spheroid to sheeting transition of immortalized human keratinocytes (HaCaT) cultured in microbubbles formed in polydimethylsiloxane,” 2011, doi: 10.1016/j.biomaterials.2011.06.013.
- [16] K. Hosseini, P. Trus, A. Frenzel, C. Werner, and E. Fischer-Friedrich, “Skin epithelial cells change their mechanics and proliferation upon Snail-mediated EMT signalling”, doi: 10.1101/2022.02.01.478626.